β - DECAY & RELATED PROCESSES

EXAMPLE OF WEAK INTERACTION

- r - PROCESS : v. n-rich nuclei decay by β-decay and form by reverse
- wk interactions set n/p ratios in changing stellar interiors :

η = neutron excess

(Iliadis §1.8)

FUNDAMENTAL VIEW OF WK INT.

quarks with interaction mediated by INTERMEDIATE VECTOR BOSONS

$m_{W^\pm} c^2 = 80$ GeV   CHARGED-CURRENT

$m_{Z^0} c^2 = 91$ GeV   NEUTRAL CURRENT

n: (ddu)   p: (uud)

$n \rightarrow p$

$$d \rightarrow u + e^- + \bar{\nu}_e$$

"Basic theory for β-decay can be developed without detailed knowledge of the form of the [weak] interaction."

PROCESSES

β^- $\quad (Z,N) \rightarrow (Z+1,N) + e^- + \bar{\nu}_e$

β^+ $\quad (Z,N) \rightarrow (Z-1,N) + e^+ + \nu_e$

energy into gas?

EC $\quad (Z,N) + e^- \rightarrow (Z-1,N) + \bar{\nu}_e$

e^- from K, L, M shells
or a free electron

PC $\quad (Z,N) + e^+ \rightarrow (Z+1,N) + \nu_e$
(where?)

and REVERSE of these processes
(where?)

{ PRINCIPLE OF DETAILED BALANCE
{ RECIPROCITY THEOREM relates

$\sigma_{\rightarrow}$ and $\sigma_{\leftarrow}$

ENERGETICS

- atomic or nuclear masses?
- electron binding energies incl.?
- Q > 0 for decay
- For $\beta^{\pm}$, $e^{\pm}$ and ν share energy

For EC, $\bar{\nu}_e$ is monoenergetic

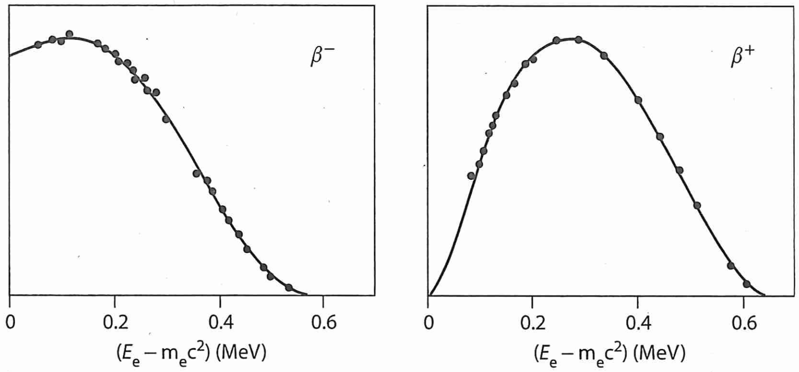

Figure 8.1 Energy distribution of the electron and positron in ^{64}Cu decay. The low energy part of the electron spectrum is enhanced due to the deceleration caused by the nuclear attraction. For the positron one has the opposite effect.

- excited states may decay differently

Table 5.1 Energy conditions in β-decay and electron capture in terms of nuclear masses, $M(Z,A)$:

Decay

β^-: $(Z,A) \Rightarrow (Z+1,A)+e^- + \bar{\nu}_e$,	$Q_\beta = (M(Z,A) - M(Z+1,A) - m_e)c^2$	$>0.$
β^+: $(Z,A) \Rightarrow (Z-1,A)+e^+ + \nu_e$,	$Q_\beta = (M(Z,A) - M(Z-1,A) - m_e)c^2$	$>0.$
EC: $(Z,A)+e^- \Rightarrow (Z-1,A) + \nu_e$,	$Q_{EC} = (M(Z,A) + m_e - M(Z-1,A))c^2$	$>0.$

In terms of atomic masses ($\mathcal{M}(Z,A)$) these conditions become:

β^-:	$Q_\beta = (\mathcal{M}(Z,A) - \mathcal{M}(Z+1,A))c^2$	$>0.$
β^+:	$Q_\beta = (\mathcal{M}(Z,A) - \mathcal{M}(Z-1,A) - 2m_e)c^2$	$>0.$
EC:	$Q_{EC} = (\mathcal{M}(Z,A) - \mathcal{M}(Z-1,A))c^2$	$>0.$

[We have assumed that the mass of the electron is equal to that of the positron. There is a fundamental theorem in relativistic quantum mechanics which is based on sound basic principles that requires particle and antiparticle to have the same mass. There is neither experimental nor theoretical reason to doubt this result.]

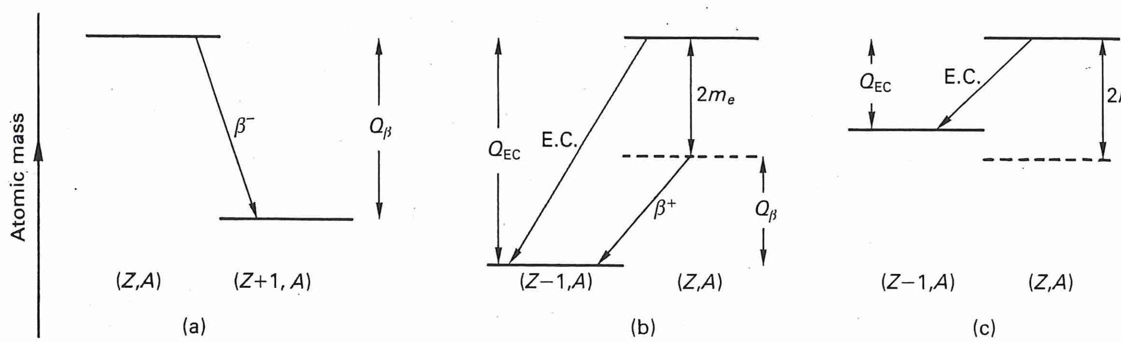

Fig. 5.5 The energy-level diagrams for β^-- β^+-decays and for electron capture (E.C.). Here it is most convenient to use a vertical scale which gives the atomic masses of the levels involved. In (a) the parent level has to be above the level of the daughter for β-decay to be possible, the level difference, Q_β, being the energy available to share among the products as kinetic energy, which, neglecting nuclear recoil, will be the maximum kinetic energy the electron can have. In (b) electron capture can occur and the mass difference (Q_{EC}) goes into total energy of the neutrino and recoil of the daughter atom (branch labelled E.C.). For β^+-decay to occur the mass difference must be greater than $2m_e$; what is left is available for kinetic energy (Q_β). This situation is represented by the right-hand branch of (b), labelled β^+. For an atomic mass difference less than $2m_e$, β^+-decay is impossible and only electron capture can occur, as shown in (c).

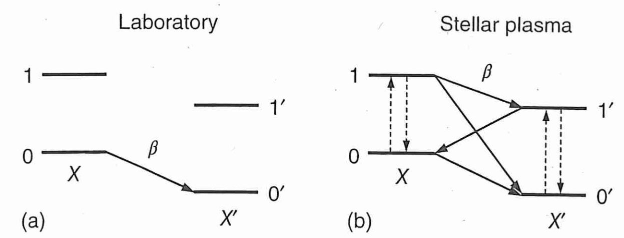

Figure 1.17 β-Decays (a) in the laboratory, and (b) in a hot stellar plasma. The vertical direction corresponds to an energy scale. For reasons of clarity, only two levels are shown in the parent nucleus X and the daughter nucleus X'. The ground and first excited state are labeled by 0 and 1, respectively. In the laboratory, the β-decay proceeds from the ground state of nucleus X to levels in nucleus X', while far more β-decay transitions are energetically accessible in a stellar plasma owing to the thermal excitation of levels (dashed vertical arrows).

Example 1.5

In the laboratory, β^+-decays of the nuclide ^{26}Al have been observed both from the ground state ($J^\pi = 5^+$) and from the first excited (isomeric) state ($J^\pi = 0^+$) located at an excitation energy of $E_x = 228$ keV (Figure 1.15). The ground state decays via positron emission to excited levels in the daughter nucleus ^{26}Mg (we will neglect a small electron capture branch) with a half-life of $T_{1/2}^{gs} = 7.17 \times 10^5$ y, while the first excited state decays to the ^{26}Mg ground state with a half-life of $T_{1/2}^{m} = 6.345$ s. Above a temperature of $T = 0.4$ GK, both of these ^{26}Al levels are in thermal equilibrium (Figure 1.16). Calculate the *stellar* half-life of ^{26}Al when the plasma temperature amounts to $T = 2$ GK.

MIXED MODES POSSIBLE

- (β^+, EC)
- (β^+, EC) & β^-
  as in ^{40}K and ^{64}Cu

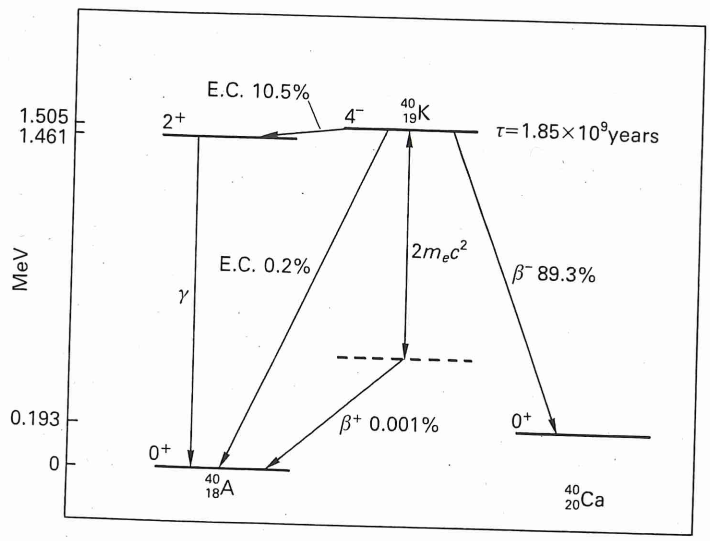

Fig. 5.8 The energy levels involved in the decay of the oo nucleus $^{40}_{19}K$ (potassium). This is an example of a nuclide with a trimodal decay: β^+, β^-, and electron capture.

- EC vs β^+ : EC gains with Z
  - $r_K \propto \frac{1}{Z}$; $v_K \propto \frac{1}{Z^3}$; overlap ↑
  - β^+ emission inhibited by Coulomb barrier & decreases with Z

EXCITED STATES

$$Q_i^* = Q_i^{GS} - E^*$$

example

$$^{29}S \rightarrow {}^{29}P + e^+ + \nu_e$$

$$^{29}S \rightarrow {}^{29}P^* + e^+ \nu$$

$$^{29}P^* \rightarrow {}^{28}Si + p$$

β-delayed proton emission

β-delayed neutron emission

" " fission

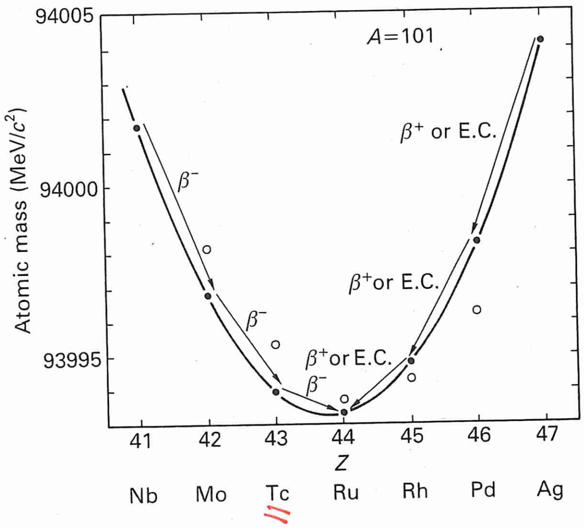

Fig. 5.6 The atomic mass of the isobars of $A = 101$ as a function of Z in the region of the line of stability. The solid points are calculated using the semi-empirical mass formula (Table 4.2); the line drawn through the points has no physical significance. The energy changes in β-decay given in Table 5.1 permit the transitions indicated so that the lowest atomic mass is thereby expected to be the only stable isobar, ruthenium in this case. This is the situation in all odd-A nuclei and the conclusion is that there is only one stable isobar for odd-A nuclei. The actual atomic masses are given by open points: the conclusion is the same. However, it is clear that even the relatively small errors in the result of the semi-empirical mass formula may not permit, in all cases, a prediction of which Z has the lowest atomic mass at the bottom of a shallow curve. For the real nuclei the transition from $A = 45$ to $A = 44$ can occur only by electron capture.

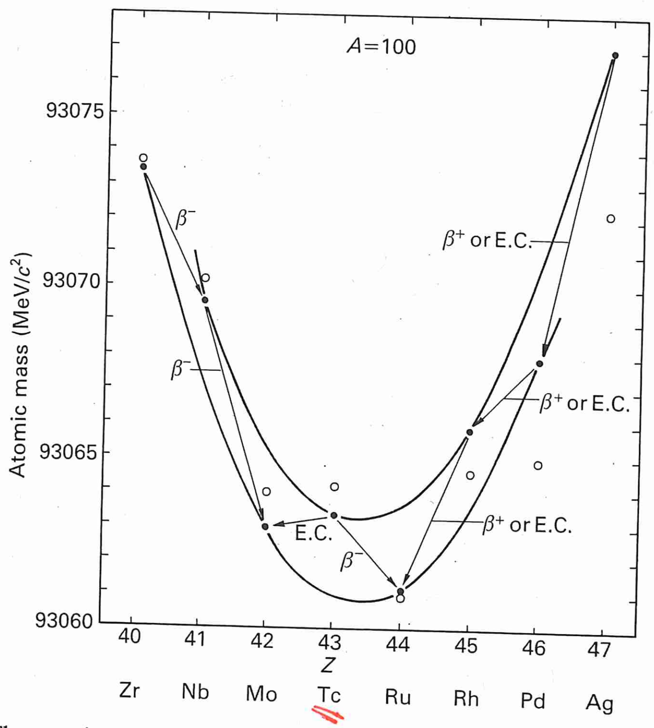

Fig. 5.7 The atomic mass of the isobars of $A = 100$ as a function of Z in the region of the line of stability. The solid points are calculated using the semi-empirical mass formula (Table 4.2). The pairing term contributes an opposite amount to the even- and odd-Z masses with the result that alternate mass points lie on different parabolae. The energy changes in β-decay given in Table 5.1 predict that the transitions indicated will occur and that molybdenum and ruthenium will be stable. As in Fig. 5.6 the actual masses are indicated by the open points. The conclusions are not changed in this case. The general conclusion is that even-A nuclei can have two or more stable isobars.

DECAY RATES

half-life $t_{1/2}$
mean life τ

$$t_{1/2} = \tau \log 2 = 0.693\,\tau$$

- measurements : 10^{-22} s to 10^{21} yrs !
  - see webposting

- theory
  - Fermi theory → "beyond scope of this book"

[Iliadis §1.8.3]

– a few remarks

Rate $\propto \int [\psi_f \, \phi_e \, \phi_\nu] \, \Omega \, \psi_i \, dV$

$$\phi_e \sim \frac{1}{\sqrt{V}} e^{\frac{i\bar{p}.\bar{r}}{\hbar}}$$

$\bar{p}$ = linear mom. of e

$$\sim \frac{1}{\sqrt{V}} \left(1 + \frac{i\bar{p}.\bar{r}}{\hbar} + \ldots \right)$$

similarly for ϕ_ν

If selection rules obeyed, retain only 1

→ ALLOWED TRANSITIONS

- NOT OBEYED, try 2^nd term

→ 1^st FORBIDDEN TRANSITIONS

- 2 — 2^nd "

3^rd "

Table 8.1 Selection rules for angular momentum and parity in β-decay.

Transition	$\Delta I = I_i - I_f$	Parity change
Allowed	$0, \pm 1$	No
First forbidden	$0, \pm 1, \pm 2$	Yes
Second forbidden	$\pm 2, \pm 3$	No
....	....	....
nth forbidden	$\pm n, \pm(n+1)$	$(-1)^n[1 = \text{yes}, -1 = \text{no}]$

$$\lambda \propto \left(G_V^2 M_F^2 + G_A M_{GT}^2\right) f(Z', E_e^{max})$$

$= \ln 2 / t_{1/2}$ (1.58)

FERMI TRANSITIONS — e, ν : opposite spin

GAMOW-TELLER TRANSITION — e, ν : parallel spins

- $f t_{1/2}$-value from expt.
- M_F^2, M_{GT}^2 challenge for theory

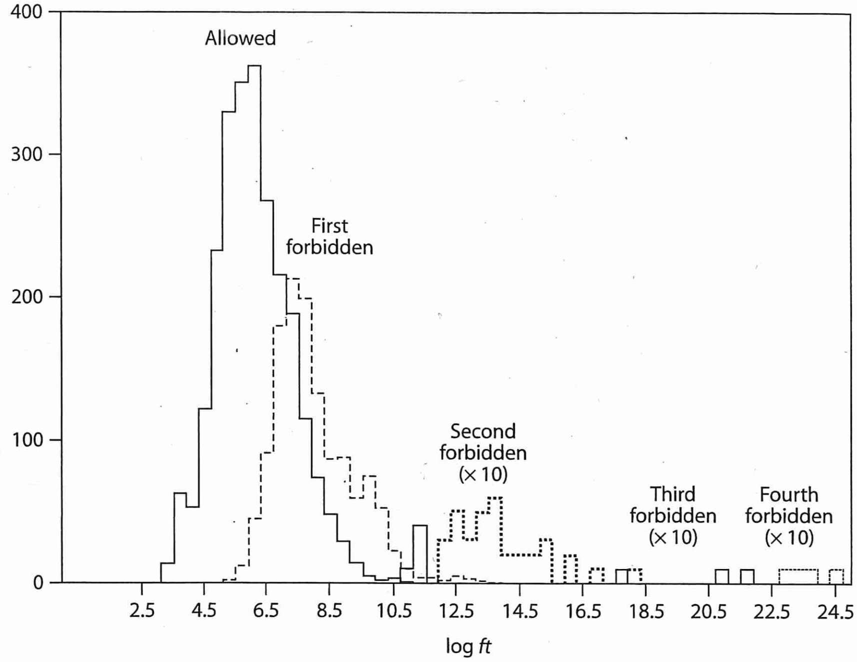

Figure 8.5 Experimental distribution of log *ft* values. The number of cases in the ordinate includes the electron capture process.

THEORY

—how good?

Sample papers to scan, even digest

G. Lorusso et al. 2015 Phys Rev Lett. 114, 192501

β-Decay half-lives of 110 neutron-rich nuclei across the N=82 shell gap

A.I. Morales et al. 2014 Phys Rev. Lett 113, 022702 Half-life systematics across the N=126 shell closure —

P Möller et al. Phys Rev. C. 67 055802 2003 New calcs of gross β-decay properties —

α - DECAY

$(A, Z) \Rightarrow (A-4, Z-2) + {}^4He$

$Q_\alpha > 0$ effectively insufficient

- COULOMB BARRIER PENETRATION

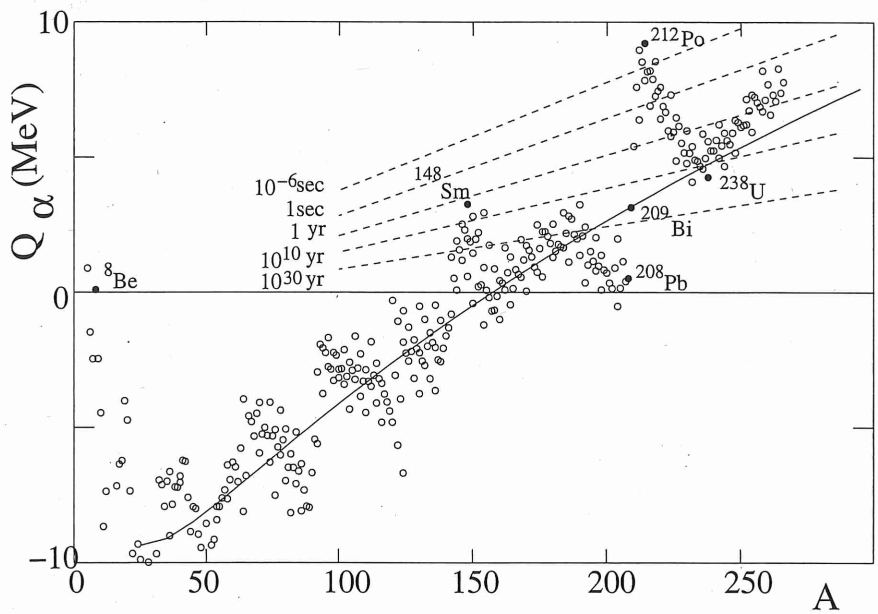

Fig. 2.14. Q_α vs. A for β-stable nuclei. The solid line shows the prediction of the semi-empirical mass formula. Because of the shell structure, nuclei just heavier than the doubly magic ^{208}Pb have large values of Q_α while nuclei just lighter have small values of Q_α. The dashed lines show half-lives calculated according to the Gamow formula (2.61). Most nuclei with $A > 140$ are potential α-emitters, though, because of the strong dependence of the lifetime on Q_α, the only nuclei with lifetimes short enough to be observed are those with $A > 209$ or $A \sim 148$, as well as the light nuclei ^{8}Be, ^{5}Li, and ^{5}He.

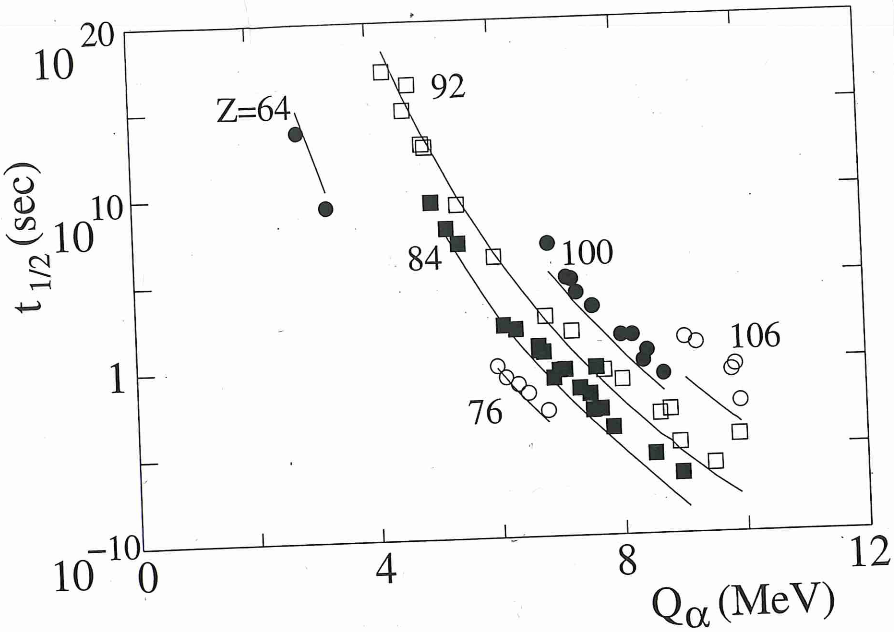

Fig. 2.15. The half-lives vs. Q_α for selected nuclei. The half-lives vary by 23 orders of magnitude while Q_α varies by only a factor of two. The lines shown the prediction of the Gamow formula (2.61).

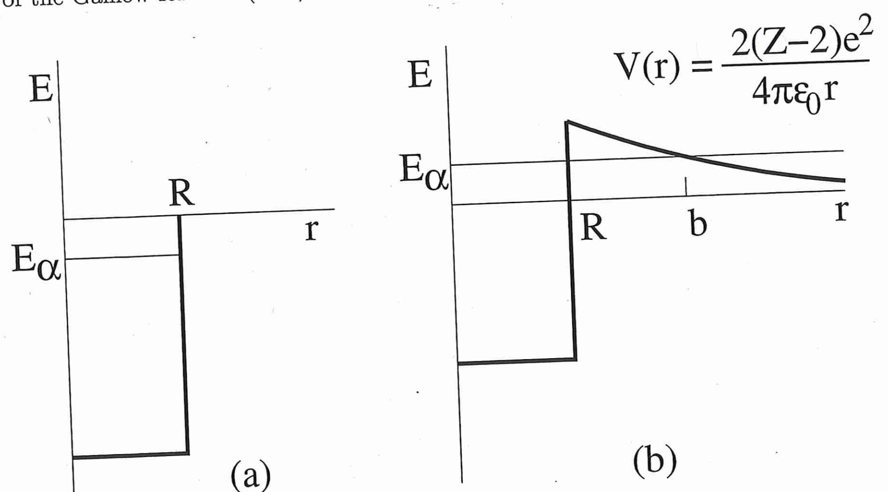

Fig. 2.16. Gamow's model of α-decay in which the nucleus contains a α-particle moving in a mean potential. If the electromagnetic interactions are "turned off", the α-particle is in the state shown on the left. When the electromagnetic interaction is turned on, the energy of the α-particle is raised to a position where it can tunnel out of the nucleus.

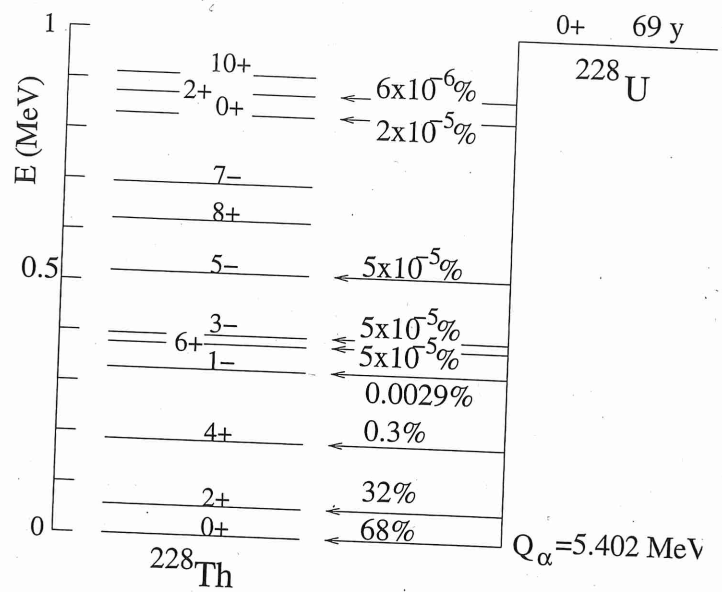

Fig. 2.17. The decay $^{228}U \rightarrow \alpha\, ^{228}Th$ showing the branching fractions to the various excited states of ^{228}Th. Because of the strong rate dependence on Q_α, the ground state his highly favored. There is also a slight favoring of spin-parities that are similar to that of the parent nucleus.

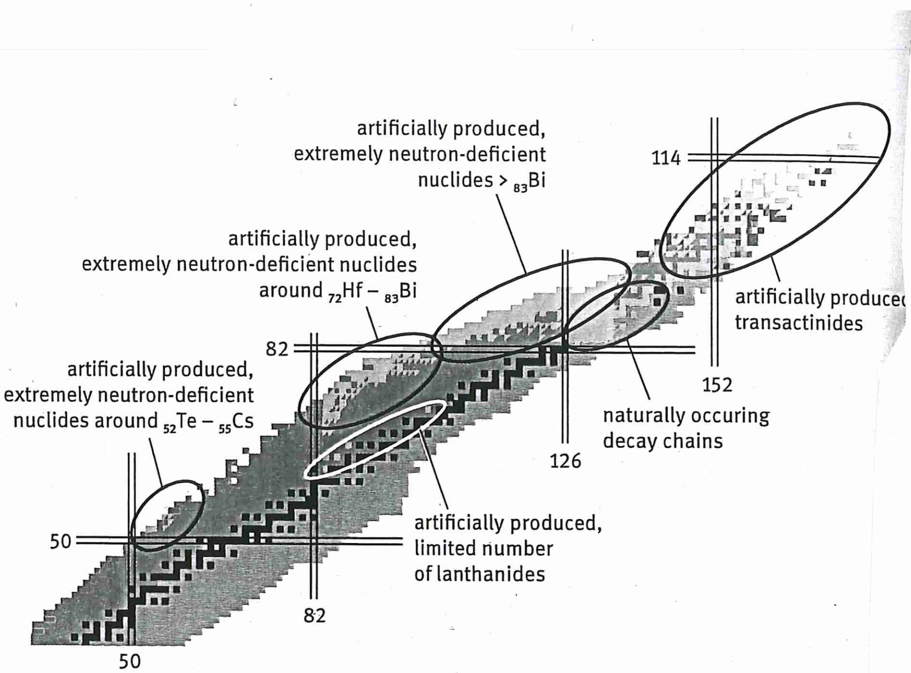

Figure 9.10: Occurrence of α-emitters within the Chart of Nuclides.

which has the solution

$$N(t) \;=\; N(t=0)\mathrm{e}^{-t/\tau}\;. \tag{4.3}$$

The mean survival time is τ, justifying its name.

The inverse of the mean lifetime is the "decay rate"

$$\lambda \;=\; \frac{1}{\tau}\;. \tag{4.4}$$

We saw in Sect. 3.5 that an unstable particle (or more precisely an unstable quantum state) has a rest energy uncertainty or "width" of

$$\Gamma \;=\; \hbar\lambda \;=\; \frac{\hbar}{\tau} \;=\; \frac{6.58\,\times\,10^{-22}\,\mathrm{MeV\ sec}}{\tau}\;. \tag{4.5}$$

Since nuclear states are typically separated by energies in the MeV range, the width is small compared to state separations if the lifetime is greater than $\sim 10^{-22}$ sec. This is generally the case for states decaying through the weak or electromagnetic interactions. For decays involving the dissociation of a nucleus, the width can be quite large. Examples are the excited states of ^{7}Li (Fig. 3.5) that decay via neutron emission or dissociation into ^{3}H^{4}He. From the cross-section shown in Fig. 3.4, we see that the fourth excited state (7.459 MeV) has a decay width of $\Gamma \sim 100$ keV.

It is often the case that an unstable state has more than one "decay channel," each channel k having its own "branching ratio" B_k. For example the fourth excited state of ^{7}Li has

$$B_{n^6\mathrm{Li}} \;=\; 0.72 \qquad B_{^3\mathrm{H}^4\mathrm{He}} \;=\; 0.28 \qquad B_{\gamma^7\mathrm{Li}} \;\sim\; 0.0\;, \tag{4.6}$$

where the third mode is the unlikely radiative decay to the ground state. In general we have

$$\sum_k B_k \;=\; 1\;, \tag{4.7}$$

the sum of the "partial decay rates," $\lambda_k = B_k\lambda$

$$\sum_k \lambda_k \;=\; \lambda\;, \tag{4.8}$$

and the sum of the "partial widths," $\Gamma_k = B_k\Gamma$

$$\sum_k \Gamma_k \;=\; \Gamma\;. \tag{4.9}$$

From Bardevant et al.

4.1.2 Measurement of decay rates

Lifetimes of observed nuclear transitions range from $\sim 10^{-22}$ sec

$$^7\mathrm{Li}\,(7.459\,\mathrm{MeV}) \;\to\; \mathrm{n}\,^6\mathrm{Li},\;\; ^3\mathrm{H}\,^4\mathrm{He} \qquad \tau \;=\; 6\times 10^{-21}\ \mathrm{sec} \tag{4.10}$$

to 10^{21} yr

^{76}Ge $\to$ ^{76}Se 2e$^-$ 2$\bar{\nu}_e$ t$_1$

It is not surprising that the tecl
siderably from one end of the sc
basic techniques, illustrated in F

- $\tau > 10^8$ yr (mostly α- and 2β-
(whose nuclei were formed ab
and isotopically isolated in n
tected. The lifetime can then
the quantity N in the sample.
Fig. 4.1.
- 10 min $< \tau < 10^8$ yr (mostly
present on Earth in significan
reactions, either artificially or
tivity sequences). The lifetim
more difficulty) isotopic purifi
(4.3) applied to derive τ. Th
the observation time is comp
necessary because τ can be de
rate.
- 10^{-10}s $< \tau < 10^3$s (mostly β-,
purification is not possible fo
nuclear reactions can be slow
material (Sect. 5.3). Decays c
Examples are shown in Figs.
state of ^{170}Yb produced in th
- 10^{-15}s $< \tau < 10^{-10}$s. (mostly
tion and decay is too short to
but a variety of ingenious tec
range that covers most of the
the fact that the time for a pa
been produced in a nuclear re
For particles with 10^{-15}s $< \tau$
chosen so that some particles
rest. For the former, the ener
and can be distinguished from
the proportion of the two ty
allows one to derive τ. The t

Another indirect techniqu
citation method. The cross-s
in collisions with a charged
3.4.2, the cross-section involv
and excited-nuclear states as
ground-state. In fact, the inci

(4.3)

ıame.
'decay rate"

(4.4)

article (or more precisely an un-
certainty or "width" of

sec (4.5)

d by energies in the MeV range,
rations if the lifetime is greater
e for states decaying through the
decays involving the dissociation
Examples are the excited states
ission or dissociation into $^3H^4He$.
e see that the fourth excited state
keV.
state has more than one "decay
ranching ratio" B_k. For example

$B_{\gamma ^7\mathrm{Li}} \sim 0.0$, (4.6)

ive decay to the ground state. In

(4.7)

$B_k\lambda$

(4.8)

$B_k\Gamma$

(4.9)

nge from $\sim 10^{-22}$ sec

$\tau = 6 \times 10^{-21}$ sec (4.10)

$$^{76}\mathrm{Ge} \rightarrow {}^{76}\mathrm{Se}\, 2e^- \, 2\bar{\nu}_e \qquad t_{1/2} = 1.6 \times 10^{21}\,\mathrm{yr} \tag{4.11}$$

It is not surprising that the techniques for lifetime measurements vary considerably from one end of the scale to the other. Here, we summarize some basic techniques, illustrated in Figs. 4.1- 4.4.

- $\tau > 10^8$ yr (mostly α- and 2β-decay). The nuclei are still present on Earth (whose nuclei were formed about 5×10^9 year ago) and can be chemically and isotopically isolated in macroscopic quantities and their decays detected. The lifetime can then by determined from (4.3) and knowledge of the quantity N in the sample. An illustration of this technique is shown in Fig. 4.1.
- 10 min $< \tau < 10^8$ yr (mostly α- and β-decay). The nuclei are no longer present on Earth in significant quantities and must be produced in nuclear reactions, either artificially or naturally (cosmic rays and natural radioactivity sequences). The lifetimes are long enough for chemical and (with more difficulty) isotopic purification. The decays can then be observed and (4.3) applied to derive τ. The case of ^{170}Tm is illustrated in Fig. 4.2. If the observation time is comparable to τ, knowledge of $N(t = 0)$ is not necessary because τ can be derived from the time variation of the counting rate.
- $10^{-10}\mathrm{s} < \tau < 10^3\mathrm{s}$ (mostly β-, γ- and α-decay). While chemical and isotopic purification is not possible for such short lifetimes, particles produced in nuclear reactions can be slowed down and stopped in a small amount of material (Sect. 5.3). Decays can be counted and (4.3) applied to derive τ. Examples are shown in Figs. 2.18 and 2.19. The case of the first excited state of ^{170}Yb produced in the β-decay of ^{170}Tm is illustrated in Fig. 4.2.
- $10^{-15}\mathrm{s} < \tau < 10^{-10}\mathrm{s}$. (mostly γ-decay). The time interval between production and decay is too short to be measured by standard timing techniques but a variety of ingenious techniques have been devised that apply to this range that covers most of the radiative nuclear decays. One technique uses the fact that the time for a particle to slow down in a material after having been produced in a nuclear reaction can be reliably calculated (Sect. 5.3). For particles with $10^{-15}\mathrm{s} < \tau < 10^{-10}\mathrm{s}$, the disposition of material can be chosen so that some particles decay "in flight" and some after coming to rest. For the former, the energies of the decay particles are Doppler shifted and can be distinguished from those due to decays at rest. Measurement of the proportion of the two types and knowledge of the slowing-down time allows one to derive τ. The technique is illustrated in Fig. 4.3.

  Another indirect technique for radiative transitions is the *Coulomb excitation* method. The cross-section for the production of an excited state in collisions with a charged particle is measured. As mentioned in Sect. 3.4.2, the cross-section involves the same matrix element between ground- and excited-nuclear states as that involved in the decay of the excited- to ground-state. In fact, the incident charged particle can be considered to be a source of virtual photons that can induce the transition. Knowledge of the cross-section allows one to deduce the radiative lifetime of the state.

- $\tau < 10^{-12}$s i.e. $\Gamma > 6 \times 10^{-10}$ MeV. (mostly γ-decay and dissociation). In this range where direct timing is impossible, the width of the state can be measured and (4.5) applied to derive τ. An example is shown in Fig. 3.4 where the energy dependence of the neutron cross-section on ^{6}Li can be used to derive the widths of excited states. In this example, the state is very wide because it decays by breakup to n^{6}Li or ^{3}H^{4}He. Widths of states that decay radiatively can only be measured with special techniques. An example is the use of the Mössbauer effect, as illustrated in Fig. 4.4.

4.1.3 Calculation of decay rates

Consider a decay

$$a \to b_1 + b_2 + \ldots + b_N \quad . \tag{4.12}$$

Particle a, assumed to be at rest, has a mass M and an energy $E = Mc^2$. As in scattering theory, we can calculate decay rates by using time-dependent perturbation theory (Appendix C). We suppose that the Hamiltonian consists of two parts. The first, H_0, represents the energies of the initial and final state particles, while the second, H_1, has matrix elements connecting initial and final states. The decay rate, i.e. the probability per unit time that a decays into a state $|f\rangle$ of final particles is

$$\lambda_{a\to f} = \frac{2\pi}{\hbar} |\langle f|T|a\rangle|^2 \, \delta_t \left(Mc^2 - \sum E_j\right) \tag{4.13}$$

where E_j is the energy of particle b_j. In first order perturbation theory, the transition operator T is just the Hamiltonian responsible for the decay, H_1.

As in the case of nuclear reactions, quantum field theory is the appropriate language to determine which decays are possible and the form of their matrix elements. Lacking this technology, we will usually just give the matrix elements for each process under consideration. However, as in reaction theory where the classical limit of particles moving in a potential was a guide for determining the matrix elements for elastic scattering, certain decay processes have classical analogs that can guide us. This is the case for radiative decays which have the classical limit of a charge distribution generating an oscillating electromagnetic field.

Despite the fact that we will not generally be able to derive rigorously the matrix elements, we can expect that the interaction Hamiltonian is translation invariant. Therefore, the square of the transition matrix element $|\langle f|T|i\rangle|^2$ will be, as in scattering theory, proportional to a momentum conserving delta function. We therefore define the "reduced" transition matrix element $\tilde{T}$ by

$$|\langle f|T|i\rangle|^2 = |\tilde{T}(\boldsymbol{p}_1 \ldots \boldsymbol{p}_N)|^2 V^{-(N+1)} \, V(2\pi\hbar)^3 \delta^3_L(\Sigma \boldsymbol{p}_j) \; , \tag{4.14}$$

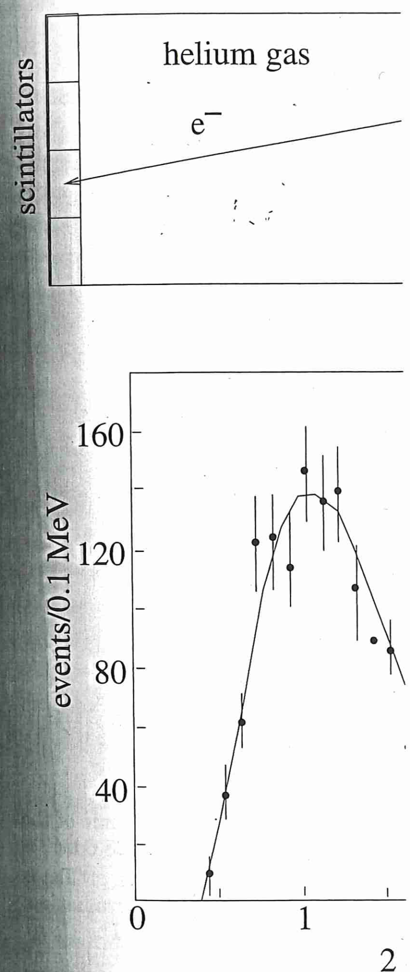

Fig. 4.1. The measurement of the d
The upper figure shows a simplified v
thick foil consisting of 172 g of isot
the natural abundance of 9.6%). Aft
foil but the decay electrons leave the
taining helium gas. The gas is instru
ionization trail left by the passing ele
The electrons then stop in plastic sci
the electron kinetic energy. The bott
electron pairs measured in this mann
a period of 6140 h, corresponding to

ı induce the transition. Knowledge of
:e the radiative lifetime of the state.
(mostly γ-decay and dissociation). In
ɔossible, the width of the state can be
e τ. An example is shown in Fig. 3.4
: neutron cross-section on ^{6}Li can be
l states. In this example, the state is
up to n^{6}Li or ^{3}H^{4}He. Widths of states
neasured with special techniques. An
effect, as illustrated in Fig. 4.4.

(4.12)

. mass M and an energy $E = Mc^2$. As
decay rates by using time-dependent
suppose that the Hamiltonian consists
ıe energies of the initial and final state
ıatrix elements connecting initial and
·obability per unit time that a decays

$$- \sum E_j) \qquad (4.13)$$

[n first order perturbation theory, the
ltonian responsible for the decay, H_1.
quantum field theory is the appropri-
ıys are possible a. . the form of their
ɔgy, we will usually just give the ma-
:onsideration. However, as in reaction
ıcles moving in a potential was a guide
r elastic scattering, certain decay pro-
guide us. This is the case for radiative
ɔf a charge distribution generating an

generally be able to derive rigorously
that the interaction Hamiltonian is
ıuare of the transition matrix element
ıry, proportional to a momentum con-
efine the "reduced" transition matrix

$$^{+1)} V(2\pi\hbar)^3 \delta^3_L(\Sigma \boldsymbol{p}_j) , \qquad (4.14)$$

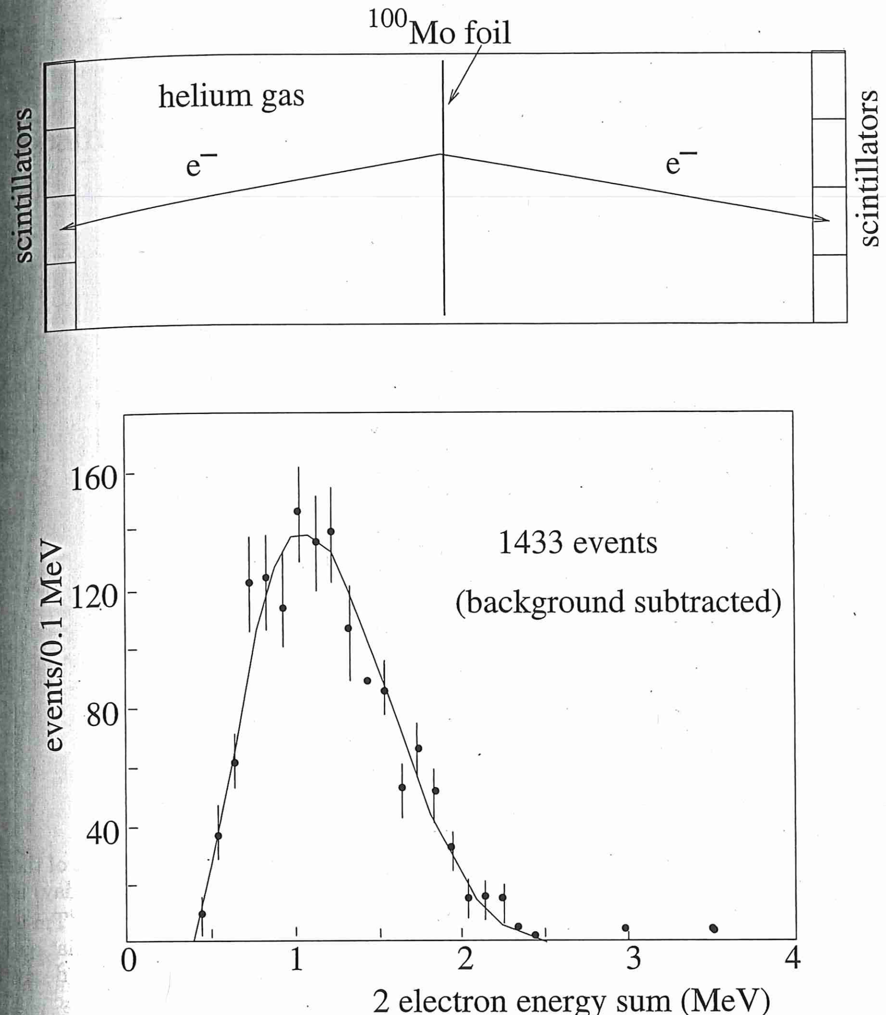

Fig. 4.1. The measurement of the double-β decay of $^{100}\text{Mo} \to {}^{100}\text{Ru}\, 2e^- 2\bar{\nu}_e$ [36]. The upper figure shows a simplified version of the experiment The source is a 40μm thick foil consisting of 172 g of isotopically enriched ^{100}Mo (98.4% compared to the natural abundance of 9.6%). After a decay, the daughter nucleus stays in the foil but the decay electrons leave the foil (Exercise 4.2) and traverse a volume containing helium gas. The gas is instrumented with high voltage wires that sense the ionization trail left by the passing electrons so as to determine the e$^-$ trajectories. The electrons then stop in plastic scintillators which generate light in proportion to the electron kinetic energy. The bottom figure show the summed kinetic energy of electron pairs measured in this manner. A total of 1433 events were observed over a period of 6140 h, corresponding to a half-life of ^{100}Mo of $(0.95 \pm 0.11) \times 10^{19}$yr.

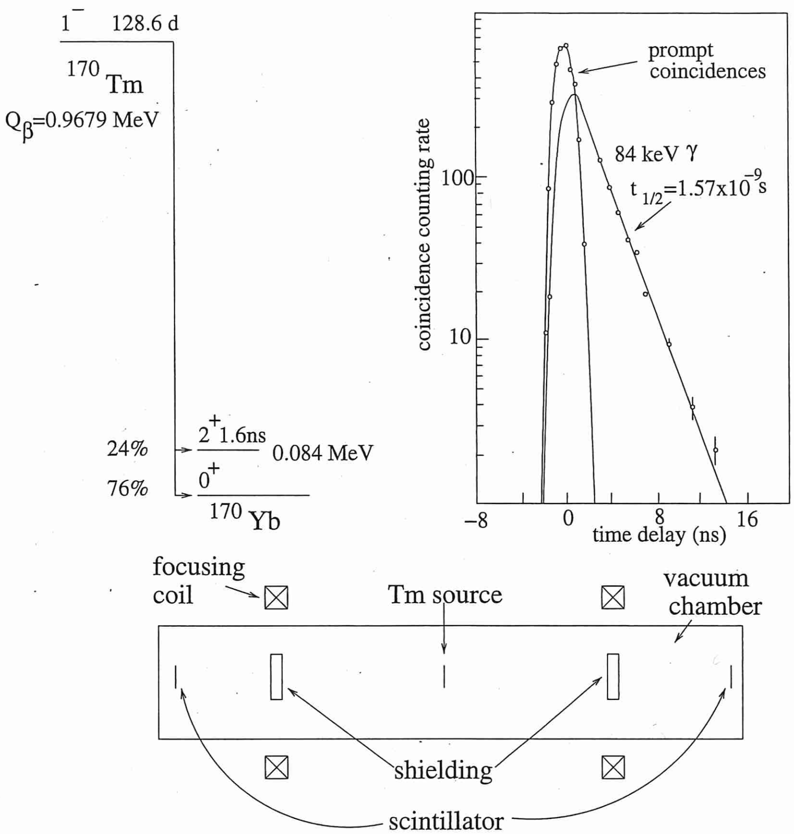

Fig. 4.2. Observation of the decay of ^{170}Tm and measurement of the lifetime of the first excited state of ^{170}Yb [37]. The radioactive isotope ^{170}Tm ($t_{1/2} = 128.6$day) is produced by irradiating a thin foil of stable ^{169}Tm with reactor neutrons. ^{170}Tm is produced through radiative neutron capture, $^{169}\mathrm{Tm}(\mathrm{n},\gamma)^{170}\mathrm{Tm}$. After irradiation, the foil is placed at a focus of a double-armed magnetic spectrometer. The decay $^{170}\mathrm{Tm} \rightarrow {}^{170}\mathrm{Yb}\,\mathrm{e}^-\bar{\nu}_e$ proceeds as indicated in the diagram with a 76% branching ratio to the ground state of ^{170}Yb and with at 24% branching ratio to the 84 keV first excited state. The excited state subsequently decays either through γ-emission or by internal conversion where the γ-ray ejects an atomic electron of the Yb. Electrons emerging from the foil are momentum-selected by the magnetic field and focused onto two scintillators. Events with counts in both scintillators are due to a β-electron in one scintillator and to an internal conversion electron in the other. The distribution of time-delay between one count and the other is shown and indicates that the exited state has a lifetime of ~ 1.57 ns.

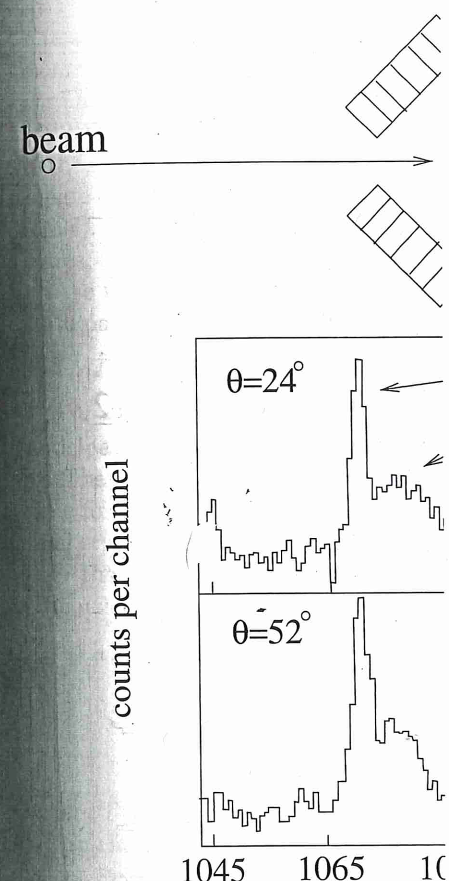

Fig. 4.3. Measurement of radiative-de
ation method" [38]. The top figure is a
measure the lifetimes of excited states of
upon a ^{58}Ni target, producing a variety
target is sufficiently thick that the proc
on the lifetime of the produced excited
("in-flight" decays) or at rest. The targ
tectors (the Euroball array) that measu
figure shows the energy distribution of
of ^{74}Br for four germanium diodes at
direction. Each distribution has two co
decays at rest and a broad tail corresp
Note that decays with $\theta > 90$ deg ($\theta > 9$
(negative). Roughly half the decays are
time necessary to stop a Br ion in the
0.25 ps for the state that decays by emis

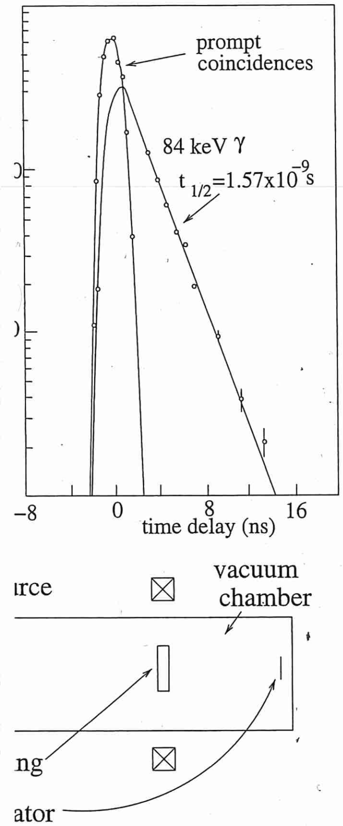

n and measurement of the lifetime of the ctive isotope ^{170}Tm (t_1 = 128.6day) is ^{169}Tm with reactor neutrons. ^{170}Tm is e, ^{169}Tm(n, γ)^{170}Tm. After irradiation, med magnetic spectrometer. The decay d in the diagram with a 76% branching h at 24% branching ratio to the 84 keV uently decays either through γ-emission ejects an atomic electron of the Yb. ntum-selected by the magnetic field and counts in both scintillators are due to a nal conversion electron in the other. The nt and the other is shown and indicates 57 ns.

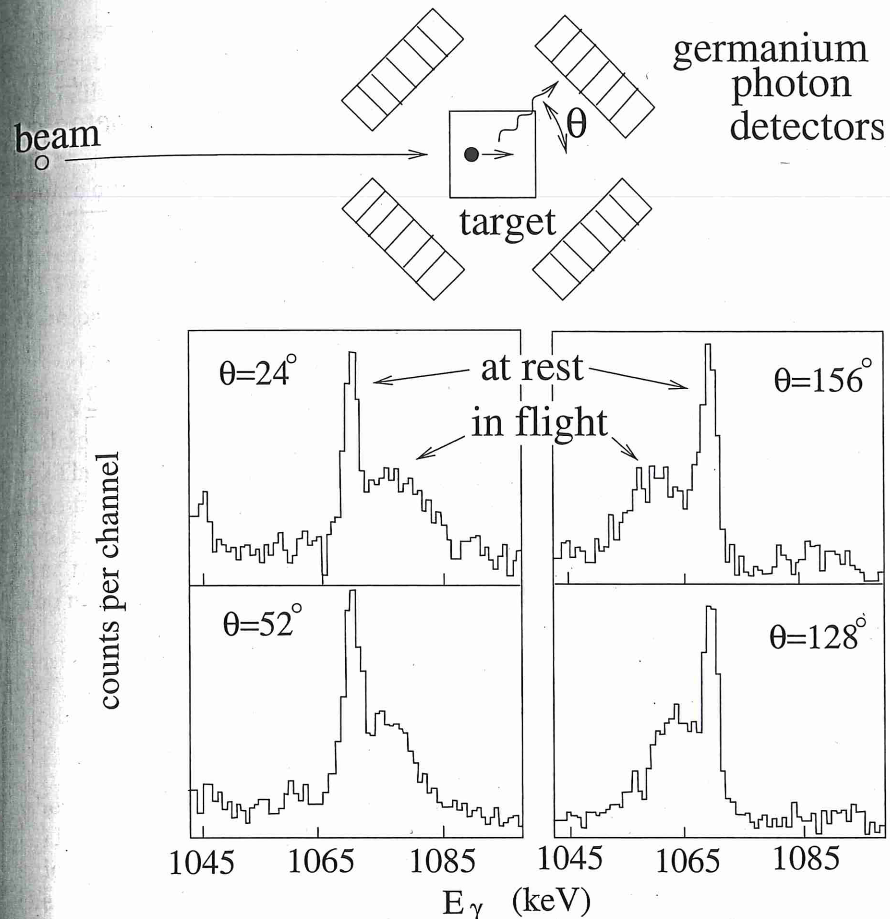

Fig. 4.3. Measurement of radiative-decay lifetimes by the "Doppler-shift attenuation method" [38]. The top figure is a simplified version of the apparatus used to measure the lifetimes of excited states of ^{74}Br. A beam of 70 MeV ^{19}F ions impinges upon a ^{58}Ni target, producing a variety of nuclei in a variety of excited states. The target is sufficiently thick that the produced nuclei stop in the target. Depending on the lifetime of the produced excited state, the state may decay before stopping ("in-flight" decays) or at rest. The target is surrounded by germanium-diode detectors (the Euroball array) that measure the energy of the photons. The bottom figure shows the energy distribution of photons corresponding to the 1068 keV line of ^{74}Br for four germanium diodes at different angles with respect to the beam direction. Each distribution has two components, a narrow peak corresponding to decays at rest and a broad tail corresponding to Doppler-shifted in-flight decays. Note that decays with $\theta > 90$ deg ($\theta > 90$ deg) have Doppler shifts that are positive (negative). Roughly half the decays are in-flight and half at-rest. Knowledge of the time necessary to stop a Br ion in the target allowed one to deduce a lifetime of 0.25 ps for the state that decays by emission of the 1068 keV gamma (Exercise 4.4).

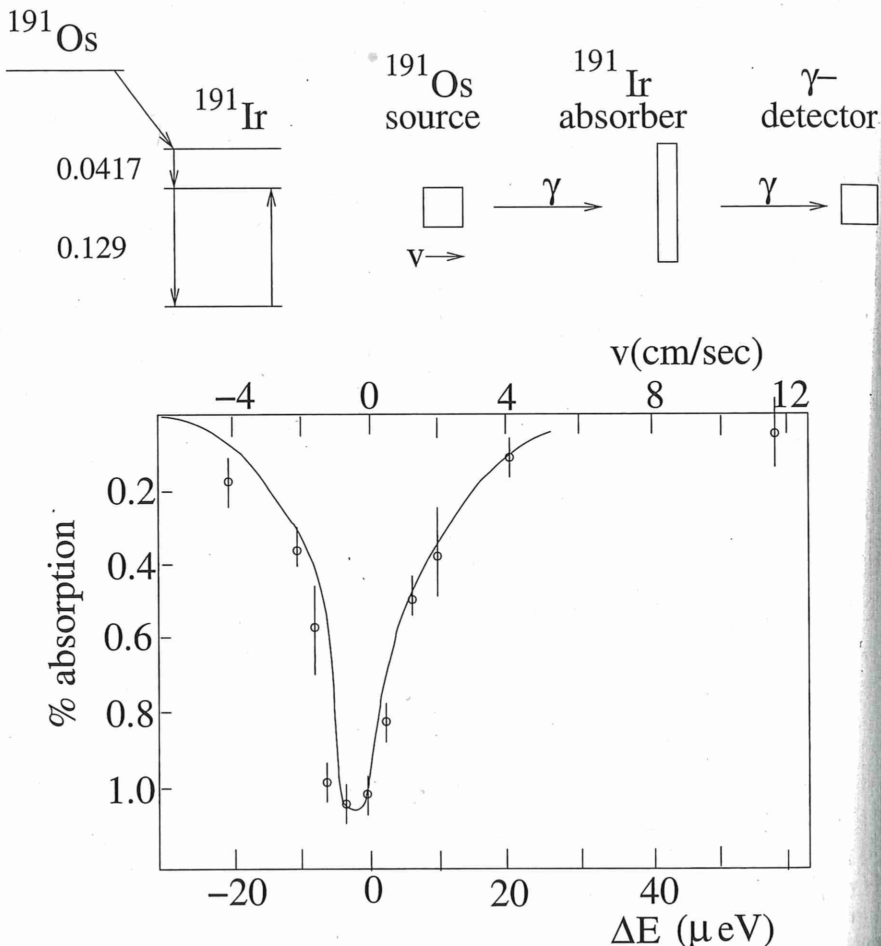

Fig. 4.4. Measurement of the width of the first excited state of ^{191}Ir through Mössbauer spectroscopy [39]. The excited state is produced by the β-decay of ^{191}Os. De-excitation photons can be absorbed by the inverse transition in a ^{191}Ir absorber. This resonant absorption can be prevented by moving the absorber with respect to the source with velocity v so that the photons are Doppler shifted out of the resonance. Scanning in energy then amounts to scanning in velocity with $\Delta E_\gamma / E_\gamma = v/c$. It should be noted that photons from the decay of *free* ^{191}Ir have insufficient energy to excite ^{191}Ir because nuclear recoil takes some of the energy (4.42). Resonant absorption is possible with $v = 0$ only if the ^{191}Ir nuclei is "locked" at a crystal lattice site so the crystal as a whole recoils. The nuclear kinetic energy $p^2/2m_A$ in (4.42) is modified by replacing the mass of the nucleus with the mass of the crystal. The photon then takes all the energy and has sufficient energy to excite the original state. This "Mössbauer effect" is not present for photons with $E > 200$ keV because nuclear recoil is sufficient to excite phonon modes in the crystal which take some of the energy and momentum.

$\tilde{T}$ represents the *dynamics* of the c
momentum conservation and stat
normalization volume $V = L^3$ ha
V-independent. The factor $V^{-(N}$
in the matrix element $(\exp(ipr)/\sqrt{}$
square of the integration over the
(C.24). The resulting factor of V
states, as demonstrated explicitly
We note that the dimensional
state particles:

$$[\tilde{T}] = \text{energy} \times \text{length}^{3(N-}$$

For $N = 3$, as in β-decay, it has
anticipate that $\tilde{T} \sim G_F$.
The reaction rate (4.12) is ob
sible final states. Just like for cro
final states in a finite volume $V =$
over the momenta of final partic
The nor alization volume cancel

$$\lambda_{a \to b_1 + b_2 \ldots + b_N}$$
$$= \frac{(2\pi\hbar)^4}{\hbar^2} \int |\tilde{T}(\boldsymbol{p}_1 \ldots \boldsymbol{p}_N)$$

where $\tilde{T}(\boldsymbol{p}_1 \ldots \boldsymbol{p}_N)$ is the reduced
In the form (4.16), the transi
sition matrix element (divided l
the accessible final states, i.e. th
momentum conservation. The qu

$$F = \int (2\pi\hbar)^4 \delta^3(\Sigma \boldsymbol{p}_j)\delta(E -$$

is called the *volume* of phase spac
decay rate (if all other factors ar
If one is interested in angular
final particles, one restricts the i
of phase space.

4.1.4 Phase space and two-b

A simple example is that of two
mass m, into a_1 and a_2 of masses
in the rest frame of a, the final r
$p \equiv p_1$. The energy of the final s